

Signature of the intermediate mass Higgs boson at the CERN LHC with flavor tagging

Pankaj Agrawal and David Bowser-Chao

Department of Physics & Astronomy, Michigan State University, East Lansing, Michigan 48824

Kingman Cheung

Center for Particle Physics, University of Texas at Austin, Austin, Texas 78712

(Received 24 October 1994)

We reexamine the exclusive signature $e^\pm(\mu^\pm) + b\bar{b}$ in the associated production of the intermediate mass Higgs boson with a W boson. We show that it is feasible to use this signature to identify the Higgs boson in the lower intermediate mass region (90 to 130 GeV) at the CERN LHC with reasonable acceptance cuts by assuming effective bottom-jet identification. We further demonstrate that the background can be reduced with judicious cuts down to the level of the signal.

PACS number(s): 14.80.Bn, 13.85.Qk, 13.85.Rm

I. INTRODUCTION

Recently the Collider Detector at Fermilab (CDF) Collaboration presented "evidence" for the existence of the top quark, estimating the top quark mass to be about 174 GeV [1]. Should this evidence turn into a firm discovery with the accumulation of further data, the Higgs boson would become the sole major missing piece of the standard model. The existence of the Higgs boson is necessary to lend support to the Higgs sector component of the standard model, which implements the symmetry-breaking mechanism that keeps the model renormalizable and gives masses to the vector bosons and fermions. In the standard model, the Higgs sector consists of a single scalar Higgs doublet and its interaction with the other fields of the model. One can extend the standard model by considering more than one Higgs doublet. However, such extensions usually include a scalar particle with properties similar to the Higgs boson of the standard model. Several nontrivial extensions of the standard model, e.g., supersymmetric models, have such an extended Higgs sector. At this moment, there does not exist any satisfactory alternative to the realization of the Higgs sector by scalar fields. Furthermore, the detectors at the CERN Large Hadron Collider (LHC) are being optimized for the detection of the standard model Higgs boson [2, 3]. It is therefore imperative that the various signatures of the Higgs boson should be studied in as much detail as possible. In this paper, we focus on one mode of detection.

There exists a lower bound on the mass of the Higgs boson of order 60 GeV from the CERN e^+e^- collider LEP [4]. It is also generally believed that if the mass of the Higgs boson is of order 1 TeV or larger, then properties of the Higgs sector will be quite different. On the basis of the production mechanisms and detection strategies, the mass of the Higgs boson can be classified as light ($M_H < M_Z$), intermediate ($M_Z < M_H < 2M_W$), or heavy ($2M_W < M_H$). In this paper, we focus on the intermediate mass region. For convenience, we further subdivide this region into two parts: the lower interme-

diate mass region ($M_Z < M_H < 130$ GeV) and the upper intermediate mass region (130 GeV $< M_H < 2M_W$).

In the intermediate mass region, the production mechanism $gg \rightarrow H$ gives rise to the largest signal rate. Over most of this mass region the dominant decay mode for the Higgs boson is $H \rightarrow b\bar{b}$. A combination of these two production and decay mechanisms would lead to two bottom jets in the final state. Unfortunately, the signal here is overwhelmed by the background due to the direct production of such jets through a strong interaction, even if bottom jets could be flavor tagged [5]. Therefore, numerous rare decay modes of the Higgs boson have been examined in the literature. It has been found that the decay mode $H \rightarrow ZZ^*$ may be useful (where Z^* is an off-mass-shell Z boson) in the upper intermediate mass region [6]. Because of the necessity of the leptonic decay of both Z bosons, however, with the expected luminosities, the number of signal events will be quite small after experimental cuts are applied. Also, this scheme will not be useful if $M_H < 130$ GeV, because the already small branching ratio for $H \rightarrow ZZ^*$ drops rapidly with M_H .

In the lower intermediate mass region, the rare decay mode $H \rightarrow \gamma\gamma$ has been found to be useful. The signal naturally peaks sharply in the invariant mass $m(\gamma\gamma)$ distribution. If one assumes both very low systematic error and very high resolution in $m(\gamma\gamma)$, the uncertainty σ in the background B count under the signal S peak is statistical and approximately equal to \sqrt{B} , and the resulting signal significance S/σ is quite high [7, 8]. Obtaining a low systematic error, however, is far from easy in this case, as the signal-to-background ratio is only of the order of 10%. Because of this low signal-to-background ratio and the large reducible backgrounds from mistagging of jets as photons, the shape and the normalization of the background continuum distribution in $m(\gamma\gamma)$ must be measured with very high precision to perform the necessary background subtraction. Another channel to search for $H \rightarrow \gamma\gamma$ is via the associated production of a Higgs boson with a W boson or a $t\bar{t}$ pair, with the subsequent decays $H \rightarrow \gamma\gamma$ and, respectively, $W \rightarrow \ell\nu$ or $t \rightarrow b\ell\nu$. The isolated charged lepton is then used

as an event trigger to significantly reduce the standard model backgrounds, resulting in an improved signal-to-background ratio. At the LHC, however, the signal rate for these production and subsequent decay modes is quite low [9].

Because of these difficulties in the case of rare decay modes, the dominant decay channel $H \rightarrow b\bar{b}$ has also been examined for the production of the Higgs boson in association with a W boson [10, 11] or a $t\bar{t}$ pair [12]. In the case of the Higgs boson production with a $t\bar{t}$ pair, one would require tagging of at least three of the bottom jets. Furthermore, at LHC energies, the rate for the associated production with a W boson is higher than production in association with a top quark pair [5]. We thus specifically reconsider

$$pp \rightarrow WHX. \quad (1)$$

The intermediate mass Higgs boson decays predominantly into a $b\bar{b}$ pair while the W boson decays into $l^\pm\nu_l$ or two jets. The decay of the W boson into two jets will result in four jets in the final state. The rate for such events cannot compete with the QCD background production of four jets, even assuming perfect bottom jet identification. The situation is better if one instead requires the leptonic decay of the W boson, but the background rate is still at least two orders of magnitude larger than the signal. However, by requiring the two jets from the signal to be initiated by bottom quarks, we could obtain a significant reduction in the backgrounds. The problem thus depends critically on bottom jet identification.

There are several ways to tag heavy quark flavor, of which we shall briefly discuss two. One technique is to look at the semileptonic decay channel of the quark. Denoting the momentum of the charged lepton (e^\pm/μ^\pm) in the plane perpendicular to the motion of the quark by $p_{l,q}^T$, we have $p_{l,q}^T < m_q/2$. The distinguishing feature of this charged lepton, as compared to that from the decay of the W , is that it is *within* a jet. If we also reject $e^\pm/\mu^\pm + jj$ events, lacking a soft lepton which satisfies $p_{l,q}^T < 1$ GeV, we will be left with a fairly clean event sample of $e^\pm/\mu^\pm + b\bar{b}$. Unfortunately, when we use the semileptonic decay channel of the bottom quark to tag it, there is a neutrino in its decay products. This means that this method of tagging will reduce the efficacy of the principal tool for reducing the background, reconstruction of the Higgs boson, due to decreased angular and energy resolution of the bottom jets.

Another tagging method is to look for a displaced vertex using a vertex detector, exploiting the relatively long lifetime of the B meson. The identification of the secondary vertex structure associated with the B meson decay is used as a tag, allowing improved reconstruction of the bottom jets, because the hadronic decay modes of the bottom quark can also be used. This method has been used at e^-e^+ colliders [13] and at the Tevatron with success [1]. Furthermore, the ATLAS Collaboration at the LHC has included a silicon vertex detector in their proposal [2].

These two tagging mechanisms were examined in the

context of the signature $e^\pm/\mu^\pm + b\bar{b}$ in Ref. [10]. There it was found that this signature may be useful if flavor tagging is done through a vertex detector. However, at the time of that study, the top quark was expected to have a small mass, and so the backgrounds from top quark production were not considered. This signature has recently been reexamined [11], where top quark production was included as a background. For maximal signal acceptance, the authors imposed only minimal cuts and assumed tagging to include the leptonic decay modes of the bottom jets, and thus also assumed a conservatively low energy resolution for the Higgs boson peak in the $m(b\bar{b})$ distribution. While 5σ significance (taking $\sigma = \sqrt{B}$) was shown to be possible, the signal-to-background ratios were quite low, on the order of 1 part in 15 for $M_H = 100$ GeV. As will be discussed below, the naive estimate of significance S/\sqrt{B} , where S and B are the number of signal and background events, does not take into account systematic errors. Assuming the systematic error to be ϵB , where B is the total number of background events in a mass bin of $m(b\bar{b})$ around M_H , the significance is more accurately given by $S/\sqrt{(\epsilon B)^2 + B}$, where the systematic and the statistical errors are added in quadrature. If the systematic error in the measurement and the background calculation of the $m(b\bar{b})$ is as high as 10%, such a low signal-to-background ratio would mean that the signal would effectively be swamped in background.

In this paper we take a different tact, emphasizing the necessity of a much higher signal-to-background ratio for clear detection, taking into account the possibly dominant systematic error. Based on the studies by the Solenoidal Detector Collaboration (SDC) [8], where displaced vertex tagging of hadronically decaying bottom jets yielded about 30% efficiency for high- p_T bottom jets, we assume energy and angular resolutions of the bottom jets to be as high as nonbottom jets. Through the improved resolution and more stringent cuts, we achieve both higher signal-to-background ratios and significance. Furthermore, we point out several other cuts that dramatically increase the signal-to-background ratio. While these cuts may reduce the naive estimate of significance, the actual signal significance may increase, depending on the level of systematic error present in the measurement.

The paper is organized as follows. In the next section, we describe the various processes that contribute to the total background. In Sec. III, we discuss the computation of and the numerical results for the signal and the various backgrounds. In this way, we assess the usefulness of the exclusive $e^\pm/\mu^\pm + b\bar{b}$ signature. In Sec. IV, we explore ways to enhance the signal-to-background ratio. In Sec. V, we present our conclusions.

II. BACKGROUND PROCESSES

The exclusive signature studied here is $e^\pm/\mu^\pm + b\bar{b}$. By exclusive, we mean that we veto any event that has extra hard particles other than an isolated charged lepton and two bottom jets. Therefore, any process that can give rise to a W boson and two bottom jets with the W

boson decaying leptonically is a background. Another source of background is due to flavor misidentification. A gluon or light-quark-initiated jet can fake a bottom jet with a small probability; we therefore also consider processes that give rise to potential backgrounds due to this misidentification.

The backgrounds include W production in association with two jets (one, both, or none of which are bottom jets):

$$pp \rightarrow Wb\bar{b}X, \quad (2)$$

$$pp \rightarrow WZX, \quad (3)$$

$$pp \rightarrow WjjX. \quad (4)$$

The QCD-induced process (2) generates a continuum background in $m(b\bar{b})$, and is more than an order of magnitude larger than the signal. Process (3) (where the Z boson decays into a pair of bottom quarks) will be peaked in $m(b\bar{b})$ around M_Z , but as a result of the intrinsic width of the Z and the finite resolution in jet energy, it will be a non-negligible background for Higgs boson masses within about 10 GeV of M_Z . The last process is a background when both jets are mistagged as bottom jets. Fortunately, the probability of a high- p_T jet faking a bottom jet is quite small, of the order of 1%. We also note that the jets from process (4) tend to have smaller p_T as compared to the signal, which will help to further reduce this background. Calculations of the cross sections and distributions for these processes already exist in literature. For processes (2), (3), and other backgrounds discussed below, we have carried out independent calculations, while for process (4) we have used an existing program [14]. Since the calculations are straightforward, we will not detail our calculations here.

The other sources of background considered here are top quark productions. Since the D0 Collaboration has placed a lower limit of 131 GeV on the top quark mass [15], above the threshold $M_W + M_b$, the top quark decays with unit probability into a W boson and bottom quark. Thus the processes listed below, which include production of one or more top quarks, can also mimic the signal:

$$pp \rightarrow t\bar{t}X, \quad (5)$$

$$pp \rightarrow t\bar{b}X, \bar{t}bX, \quad (6)$$

$$pp \rightarrow t\bar{q}X, \bar{t}qX, \quad (7)$$

$$pp \rightarrow t\bar{b}qX, \bar{t}bqX. \quad (8)$$

The strong-interaction process (5) is the primary mechanism for top quark production at the hadron colliders. It poses as a background to the electroweak signal in two ways. The top quark can decay either semileptonically or hadronically, i.e., $t \rightarrow b\ell\nu_\ell$ or $bq\bar{q}'$. Since our signature requires one isolated charged lepton, either the top quark or the top antiquark must decay semileptonically, while the other can decay either way. If one top quark decays hadronically and the other leptonically, there will be two light quark jets in the final state in addition to the charged lepton and the bottom jet pair. Because the top quarks are very heavy and produced at central ra-

pidities, the extra jets from the top decay will tend to have large p_T in the central rapidity region. Similarly, if both top quarks decay leptonically, the extra lepton will be stiff and central. Either way, we can reduce the top pair background by vetoing extra leptons or jets to as low p_T and as large rapidity as covered by detectors. Here and in all our calculations but the Wjj program, we have included full spin correlations in the decay of top quarks and W bosons.

Processes (6)–(8) involve electroweak production of a single top quark. In these processes, the top quark must decay semileptonically to give the charged lepton. Process (6) is, like the signal, produced through the Drell-Yan mechanism. Despite its strong similarity to the signal, we shall see in Sec. IV that there do exist methods to enhance the signal with respect to this background. Process (7), which is obtained from the Feynman diagrams of process (6) by crossing, requires a mistag of the light outgoing quark. Finally, the process (8) mainly comes from gluon- W fusion. The extra quark in process (8) is mostly produced at forward rapidities, thus making this background difficult to suppress. As with the top pair background, vetoing extra final state particles (in this case, the light quark jet) is the most effective cut. In fact, we have required the signal to be exclusive mainly in order to reduce these top production backgrounds.

We have computed the cross sections for all processes at the tree level for consistency; in any case, the QCD corrections are not available for all the backgrounds considered. The question thus arises as to the effect of these next-to-leading order (NLO) corrections. *A priori*, it is possible that the inclusion of QCD corrections may require a significant modification in our signature and the sets of cuts that we consider to achieve the observability of the signal. The QCD corrections to the signal production have been calculated, and found to be about 10–15% [16, 17]. In the case of backgrounds, depending on the process, the corrections could range from 10% to 50% [18]. Therefore, if we were examining an inclusive signature, we would expect the number of background events to increase more than that of the signal, which could lead to a decrease in the significance. However, we will argue that higher-order QCD corrections will not significantly affect the kinematics of the final state particles for the signal and backgrounds in our analysis. Therefore, our set of judicious cuts should also be applicable when higher QCD corrections are taken into account.

Since we are examining an exclusive signature, the issue of initial state radiation is especially important. As remarked above, the exclusive nature of the signal serves to cut down two major backgrounds: $pp \rightarrow t\bar{t}X$ and $pp \rightarrow t\bar{b}qX, \bar{t}bqX$. In Sec. IV, we impose an extra lepton and/or jet veto to the maximum coverage allowed by the detector, i.e., the minimum $p_T(\ell/j)$ and maximum pseudorapidity $|\eta(\ell/j)|$. At the tree level, this cut has no apparent effect on the signal; on the other hand, Altarelli-Parisi evolution of the parton distribution functions implies that the hard scattering process will necessarily be accompanied by extra jets, whose energy scale should be small compared to the hard scattering energy scale. Because this scale is of order $M_H + M_W \approx 200$ GeV, we

expect a significant fraction of the signal and background events to include one or more extra jets of $p_T \gtrsim 15$ GeV.

As is well known, the NLO calculation is an unreliable measure of the frequency of this extra radiation; we expect an estimate based on fixed-order perturbation theory to break down below a certain value of p_T for the extra jet. Resummation indicates where this breakdown takes place; for the signal at the LHC, one expects this minimum p_T to be around 25–30 GeV [17]. Resummation, in turn, does not offer any information about the number of extra soft jets or their individual p_T ; so to help answer these questions, we have employed a Monte Carlo generator (PYTHIA [19]).

This type of Monte Carlo simulation usually includes only bremsstrahlung-type corrections; inclusion of loop corrections in a consistent manner has been implemented in some specialized Monte Carlo generators in the case of a very few processes. However, our interest is in that part of NLO corrections that gives rise to extra soft jets, for which purpose PYTHIA can serve fairly well (though we note that the total cross sections calculated by such programs are normalized to LO only, thus necessitating multiplying results by an overall K factor).

To show that our analysis would not be significantly altered by the inclusion of NLO corrections, we have carried out a simple study using PYTHIA. The results discussed at the end of the next section essentially imply that our veto of extra jets may be modified slightly so as to allow for about the same signal event rate as obtained with our cuts on the NLO cross sections, while sufficiently suppressing processes (5) and (8).

III. NUMERICAL RESULTS

In this section, we present the signal and background event rates at the LHC. Because the collider and its de-

tectors are not expected to become operational for almost a decade, actual detector resolution and efficiency are of course still uncertain; for our study, we have employed a simple detector simulation based on the parameters presented in the ATLAS Collaboration's letter of intent (LOI) [2].

To bracket the range of detector performance of the ATLAS Collaboration, we consider two scenarios. The first scenario is for more optimistic detector performance, while the second scenario assumes more conservative detector acceptance. In addition, the differences between the two scenarios include the efficiency assumed for tagging the b quarks and in the veto for extra final state particles. Explicit details are summarized in Table I. We assume the same hadronic and lepton Gaussian energy resolutions for both scenarios (also given in the table and taken from the ATLAS LOI). As part of the cuts outlined below, we veto an event if an extra electron or muon is detected in the central region; in the forward region ($3 < |\eta| < 4.5$), we rely on the hadronic calorimeter to detect and veto electrons (but not muons). No angular resolution effects have been included. The missing transverse energy \cancel{E}_T is calculated by adding up all the visible (smeared) momenta and assuming hermetic coverage of soft forward radiation.

Because of large hadronic backgrounds at the LHC and because our signature involves two bottom jets, it is clear that b tagging is crucial. B tagging is characterized both by true b -jet tagging efficiency and light quark and/or gluon mistagging rates. Studies by the SDC [8] and ATLAS [2] Collaborations estimated b tagging through displaced vertices to have an efficiency of about 30% and a mistagging rate of 1% for jets of $p_T \gtrsim 40$ GeV, with degraded b -tagging efficiency for lower- p_T jets due to the correspondent decrease in impact parameter resolution. We have taken these efficiencies to be independent of

TABLE I. Acceptance and cut parameters, based on the ATLAS detector, for two scenarios: (i) optimistic and (ii) conservative.

Acceptance and cut parameters	Scenarios	
	(i) Optimistic	(ii) Conservative
Energy resolution ($\Delta E/E$):		
central e/μ ($ \eta < 3$)	10/ \sqrt{E} % \oplus 1%	
central jets ($ \eta < 3$)	50/ \sqrt{E} % \oplus 3%	
forward jet/ e ($3 < \eta < 4.5$)	100/ \sqrt{E} % \oplus 7%	
max $ \eta(b) $	2	2
min $p_T(b)$	20 GeV	30 GeV
min $\Delta R(b, \bar{b})$	0.6	
b-tagging efficiency	30%	
non- b -jet acceptance	1%	
Higgs reconstruction	$ m(b\bar{b}) - M_H < 7.5$ GeV	
max $ \eta(e/\mu) $	3	2.5
min $p_T(e/\mu)$	10 GeV	15 GeV
min $\Delta R(b, e/\mu)$	0.6	
max $m_T(e/\mu, \nu)$	80 GeV	
Veto efficiency for jet/ e with 15 GeV $< p_T(\text{jet})$, $ \eta(\text{jet}) < 4.5$	100%	
Veto efficiency for jet/ e with 10 GeV $< p_T(\text{jet}) < 15$ GeV, $ \eta(\text{jet}) < 4.5$	100%	50%

p_T , but for the more conservative scenario (ii), we require a higher minimum p_T than in the more optimistic scenario (i). Finally, we take the energy resolution of the bottom jets to be that of ordinary jets, because we are relying on displaced vertices for b tagging instead of soft, nonisolated leptons and their concomitant neutrino(s). Furthermore, since the fragmentation of the bottom jets is expected to be harder than for nonbottom jets, one would expect the bottom jet energy resolution to be somewhat better than for light quarks or gluon jets.

Table I shows that the acceptance cuts for the tagged lepton are tighter in the second scenario than the first one. The larger pseudorapidity coverage in scenario (i) is not unreasonable, however, assuming that tagging of either of the two bottom jets can serve as efficiently as the lepton tagging for an event trigger. With regard to the minimum p_T , the LOI indicates that coverage as low as 6–10 GeV should be considered; if a more detailed study showed sizable lepton backgrounds from heavy flavor decay, one could employ the more stringent cuts of scenario (ii). As explained above, the transverse mass cut is imposed to ensure consistency with the presence of a W boson. For the purpose of this cut, in both scenarios we have included forward ($|\eta| > 3$) muons as a source of \cancel{E}_T .

The most significant difference between the two sets of cuts is the treatment of vetoing extra particles. According to the ATLAS LOI, the rapidity coverage of the hadronic calorimeter is expected to be up to 5. The central issue for forward jet/ e vetoes is thus to what minimum p_T value these jets will be visible. We emphasize that we are not assuming precision measurement of forward, soft jets, since these jets are not part of our signal. Any observation of a forward jet would suffice, as long as the underlying event for each signal event did not mimic such jets very frequently. In any case, in both scenarios we assume 100% efficiency for tagging jets and/or electrons of $p_T > 15$ GeV within the active region of the calorimeter ($|\eta| < 4.5$), and for scenario (ii) we take a reduced efficiency of 50% for jets and/or electrons with $10 \text{ GeV} < p_T < 15 \text{ GeV}$ in the same rapidity range.

Before presenting results for the two scenarios, we briefly describe the inputs to our calculation. First, we have conservatively assumed a yearly LHC integrated luminosity of 10 fb^{-1} . Although the luminosity is eventually expected to grow by a factor of 10–50 larger, it is quite possible that only the nominal luminosity will be attainable in the first few years of operation. Furthermore, while the rate for overlapping b -tagged events (with accompanying tagged leptons) at a much higher luminosity is not expected to pose a problem, it is not clear whether a silicon vertex detector would be able to survive such an environment. Because all the processes were calculated here to leading order, we employed the CTEQ2 set 5 distributions [20], which are leading order fits. Similarly, α_s is calculated to leading order with the value of Λ_{QCD} given by the parton distributions. The factorization and/or renormalization scales were selected as follows. For the two s -channel processes (WH and tb production), we took $Q^2 = \hat{s}$. For the others, which were at least in part t -channel processes, we took $Q^2 = \hat{s}/4$.

Though the cross sections demonstrate a dependence on the choice of this scale [most notably process (5)], only if all the next-to-leading order calculations are available could the scale dependence be reduced. In their absence, we have used a representative scale for each of the processes, taking into account the nature of the exchange involved. However, reasonable variations in the factorization and/or renormalization scale are not expected to significantly alter the results for the significance and the signal-to-background ratio.

We present our results for the two scenarios in Tables II–V. As can be seen, in both scenarios we can achieve very good statistical significance S/\sqrt{B} (where we for the moment ignore systematic errors). One would therefore expect the signature under consideration to serve quite well as a detection mode. For $M_t = 175$ GeV, for example, over most of the lower intermediate mass range one can obtain a significance of 4 or higher for 10 fb^{-1} integrated luminosity. For $M_H \approx 90$ GeV the worst backgrounds are $Wb\bar{b}$ and WZ , the latter of which drops substantially as M_H increases from 90 GeV. For the other Higgs boson masses, the largest backgrounds are $Wb\bar{b}$ and $t\bar{t}$ for a smaller top mass $M_t \lesssim 175$ GeV, but for a larger top mass $M_t \gtrsim 175$ GeV, tbq and $Wb\bar{b}$ backgrounds are the most serious. Through our strategy of requiring an exclusive signature, we have succeeded in reducing the top pair and tbq backgrounds to an acceptable level. A fairly high minimum p_T for the bottom jets has also worked rather well in decreasing the Wjj background relative to the signal, as can be seen from comparing the results of the two scenarios. This is expected as the jets in Wjj are mainly bremsstrahlung gluons off quark or gluon lines.

TABLE II. Event rates for optimistic scenario (i) (see Table I) at the LHC, assuming 10 fb^{-1} of yearly integrated luminosity. For the top quark backgrounds, the top quark mass begins each respective row.

Processes	M_H	M_H	M_H	M_H
	90 GeV	100 GeV	110 GeV	120 GeV
WH	155.6	116.6	86.8	59.7
Wjj	101.6	90.4	75.3	58.1
$Wb\bar{b}$	198.7	154.7	122.7	98.3
WZ	165.8	84.2	8.7	2.5
$t\bar{t}$				
150 GeV	116.1	113.4	106.8	101.0
175 GeV	45.3	45.1	45.7	46.5
200 GeV	17.5	19.0	20.2	20.5
tbq				
150 GeV	75.5	68.3	59.4	49.6
175 GeV	63.4	59.3	53.2	47.1
200 GeV	52.2	53.0	46.9	45.2
tb				
150 GeV	75.0	70.7	70.2	66.4
175 GeV	34.8	38.9	38.5	36.5
200 GeV	17.8	19.7	21.1	19.9
tq				
150 GeV	35.8	36.9	36.9	37.7
175 GeV	23.8	25.3	26.6	27.9
200 GeV	15.3	17.4	18.4	19.6

TABLE III. Scenario (i): Signal statistical significance and years required for 5σ detection, assuming 10 fb^{-1} of yearly integrated luminosity.

Scenario (i) optimistic	M_H	M_H	M_H	M_H
	90 GeV	100 GeV	110 GeV	120 GeV
$M_t = 150 \text{ GeV}$: S/B	155.6/768.5	116.6/618.6	86.8/480.0	59.7/413.6
	Significance	5.6	4.7	4.0
	years for 5σ detection	0.8	1.1	1.6
$M_t = 175 \text{ GeV}$: S/B	155.6/633.4	116.6/497.9	86.8/370.7	59.7/316.9
	Significance	6.2	5.2	4.5
	years for 5σ detection	0.7	0.9	1.2
$M_t = 200 \text{ GeV}$: S/B	155.6/568.9	116.6/438.4	86.8/313.3	59.7/264.1
	Significance	6.5	5.6	4.9
	years for 5σ detection	0.6	0.8	1.0

The cuts of the two scenarios were selected for their effect on the significance, ignoring the signal-to-background ratio. In the next section, we shall discuss strategies to help in reducing the signal-to-background ratio, which would be crucial in the event that systematic errors dominate the background uncertainty.

We now explore the consequences of considering the NLO corrections to the cross sections and the kinematics of the signal and background events. As discussed in Sec. II, we do so through a simple simulation employing PYTHIA. The focus was on investigating the necessary modifications to our simple “extra jet and/or lepton” veto that would retain a large fraction of the signal while still sufficiently suppressing the $t\bar{t}$ and tbq backgrounds.

We included initial state radiation (but no final state radiation or hadronization) to study the differences between initial state radiation in the signal and in the backgrounds. Setting the threshold for extra jets at $p_T > 15 \text{ GeV}$, we find that about 40% of the signal events have one or more extra jet in the central rapidity region, with the bulk of such events containing only one extra jet. Thus our simple veto of as few as one extra jet would cut by more than a third the signal acceptance (including the NLO normalization). The top pair background was accompanied by extra jets about 60–70% of the time. For the other background processes we expect similar rates for extra jets.

Allowing up to one extra jet, and vetoing an event only if it had *two* or more extra jets would yield a higher signal acceptance and help to reduce the high-jet-multiplicity top pair background, but leave the tbq background untouched at LO. Fortunately, it turns out that the extra jet in the case of the signal tends to be soft — to pass the minimal p_T cut of 15 GeV, the jet is quite central and with an energy not much larger than its transverse momentum. For $pp \rightarrow t\bar{b}qX, \bar{t}bqX$, in contrast, the extra jet to be vetoed has both large p_T and large energy. By vetoing events with a single extra jet having either $p_T > 50 \text{ GeV}$ or $E > 150 \text{ GeV}$, this background is suppressed to about the same extent as in scenario (ii), with signal acceptance on par with our LO estimates and cuts. The top pair background tends to be accompanied by three or more extra jets, and so even this relaxed jet veto will drastically reduce this background. We estimate that inclusion of events with one extra jet would enhance the

top pair background at most by 50–75%, which represents less than 10% increase in the total background rate.

Finally, we emphasize that though this preliminary study indicates that (with the inclusion of the NLO corrections) our modified cuts will likely lead to a comparable signal acceptance and signal-to-background ratio, a full study of all the processes, including initial and final state radiations, will be a necessary check of these results.

IV. ENHANCING SIGNAL TO BACKGROUND

The cuts presented in the previous section were of two types: acceptance cuts and significance-enhancing cuts. Acceptance cuts were just those made to ensure the visibility of the signal, regardless of the background

TABLE IV. Event rates for the more conservative scenario (ii) (see Table I) at the LHC, assuming 10 fb^{-1} of yearly integrated luminosity. For the top quark backgrounds, the top quark mass begins each respective row.

Processes	M_H	M_H	M_H	M_H
	90 GeV	100 GeV	110 GeV	120 GeV
WH	101.5	83.9	66.7	48.2
Wjj	44.8	42.9	41.3	37.6
Wbb	119.6	104.5	89.7	75.3
WZ	97.1	52.0	5.8	1.8
$t\bar{t}$				
150 GeV	84.2	87.2	90.0	84.2
175 GeV	34.0	38.5	38.0	37.6
200 GeV	14.0	16.7	17.5	17.8
tbq				
150 GeV	49.3	53.2	46.8	43.1
175 GeV	38.2	42.8	42.9	41.8
200 GeV	29.8	34.7	36.6	37.6
$t\bar{b}$				
150 GeV	49.6	52.0	53.7	50.8
175 GeV	23.4	26.0	28.6	28.9
200 GeV	12.6	14.5	16.0	16.6
tq				
150 GeV	21.2	24.3	25.9	26.2
175 GeV	13.9	16.4	18.2	19.9
200 GeV	8.8	10.7	12.6	13.9

TABLE V. Scenario (ii): Signal statistical significance and years required for 5σ detection, assuming assuming 10 fb^{-1} of yearly integrated luminosity.

Scenario (ii) conservative	M_H	M_H	M_H	M_H	
	90 GeV	100 GeV	110 GeV	120 GeV	
$M_t = 150 \text{ GeV}$: S/B	101.5/465.8	83.9/416.1	66.7/353.2	48.2/319	
	Significance	4.7	4.1	3.5	2.7
	years for 5σ detection	1.1	1.5	2.0	3.4
$M_t = 175 \text{ GeV}$: S/B	101.5/371	83.9/323.1	66.7/264.5	48.2/242.9	
	Significance	5.3	4.7	4.1	3.1
	years for 5σ detection	0.9	1.1	1.5	2.6
$M_t = 200 \text{ GeV}$: S/B	101.5/326.7	83.9/276	66.7/219.5	48.2/200.6	
	Significance	5.6	5.1	4.5	3.4
	years for 5σ detection	0.8	1.0	1.2	2.2

acceptance, such as requiring minimum transverse momenta for the lepton and bottom quarks. Significance-enhancing cuts included the extra lepton and jet vetoes, and the requirement that the bottom quark pair closely reconstruct the Higgs boson. These cuts were intended to maximize the naive estimate of the signal significance, S/\sqrt{B} , where we ignored the effect of systematic error.

In practice, of course, a systematic error could be relatively important. We have performed a background subtraction to obtain the various values for the significance given in the previous section, where we assumed accurate measurement of the background over some reasonable range in $m(b\bar{b})$. Aside from the theoretical uncertainty in the various backgrounds, the relatively low event rates for the background (with all but the Higgs boson reconstruction cut applied) and the difficulty in reconstructing bottom jets would certainly imply some systematic error in this measurement. Given that the highest signal/background ratio in scenario (ii) was only about 1 part in 4, as discussed in Sec. I, it is important to seek additional cuts that can increase the signal-to-background ratio, which in practice could be the true figure of merit. In this section, we examine several such cuts. For the sake of simplicity, we will present results for typical top quark and Higgs boson masses at $M_t = 175 \text{ GeV}$, $M_H = 100 \text{ GeV}$, and starting with the cuts in scenario (ii).

As with most of the rest of this study, we are considering leading order effects only — radiative corrections can affect the practical efficacy of these cuts. The physical differences between the signal and various backgrounds are, however, most apparent at leading order, and our results should suggest analogous cuts for more detailed future studies that include initial and final state radiations, b fragmentation, etc.

From Tables II and IV, we see that direct W and top production each make up a significant portion of the total background. Considering first the W production processes, we have found the spatial separation between the bottom quark and antiquark, measured in various ways, to be quite useful. As previously reported [21], for example, the variable $\Delta R(b, \bar{b})$ defined by $\Delta R(b, \bar{b}) = \sqrt{(\Delta\eta)^2 + (\Delta\phi)^2}$, where $\Delta\eta$ is the difference in pseudorapidity and $\Delta\phi$ is the difference in azimuthal angle between b and \bar{b} , is very useful in reducing

these backgrounds. The signal is roughly flat in the range $1 < \Delta R(b, \bar{b}) < \pi$, while the W production backgrounds peak towards $\Delta R(b, \bar{b}) = \pi$. It turns out that this cut may be replaced by a simpler one in $\cos \Delta\phi(b, \bar{b})$, which is the cosine of the azimuthal angle between b and \bar{b} . Figure 1 shows a clear concentration of the W backgrounds towards $\cos \Delta\phi(b, \bar{b}) = -1$, i.e., where the jets are back to back in the transverse plane. Though not shown separately, the Wjj and $Wb\bar{b}$ are responsible for this difference from the signal; the WZ background is much more similar to the signal. This behavior reflects two characteristics of these backgrounds. Because the Wjj and $Wb\bar{b}$ backgrounds tend to have low $m(b\bar{b})$, it is easiest for them to reconstruct the Higgs boson with a minimum of energy, by producing the $b\bar{b}$ pair back to back. Because of the t -channel enhancement (of all three processes), in the center-of-mass frame of the $W + b\bar{b}$ system, the bottom quark pair is produced predominantly in the forward and/or backward regions. In the laboratory frame, the combination of these effects manifests itself as a strong peak at $\cos \Delta\phi(b, \bar{b}) = -1$.

Unfortunately, the backgrounds from top quark production do not differ significantly from the signal in this distribution. Imposing the severe cut of $\cos \Delta\phi(b, \bar{b}) > 0.5$ (Table VI) increases S/B by a factor of 1.5, though

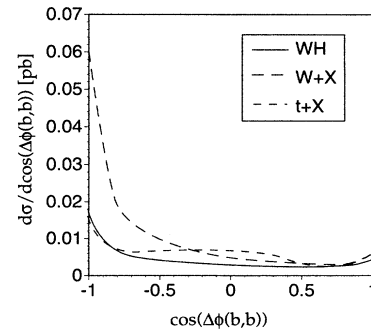


FIG. 1. The differential cross section $d\sigma/d\cos \Delta\phi(b, \bar{b})$ versus $\cos \Delta\phi(b, \bar{b})$ for $M_t = 175 \text{ GeV}$ and $M_H = 100 \text{ GeV}$ at the LHC, for the signal (solid curve), the sum of W backgrounds (dashed curve), and the sum of top quark backgrounds (dotted curve). The acceptance cuts are according to scenario (ii).

TABLE VI. The effect of S/B -enhancing cuts on the signal and the background, for $M_t = 175$ GeV, $M_H = 100$ GeV, in events per year (assuming 10 fb^{-1} of yearly integrated luminosity).

S/B -enhancing cuts imposed	$pp \rightarrow WH + X$	$pp \rightarrow W + X$	$pp \rightarrow t + X$	S/B
No additional cuts	83.9	205.0	123.7	0.26
$\cos \Delta\phi(b, \bar{b}) > 0.5$	14.0	19.0	18.5	0.37
$ z_{c.m.}^{\text{recon}}(H) < 0.4$	48.9	73.0	71.1	0.34
$ z_{c.m.}^{\text{recon}}(H) < 0.4, M_{Wb\bar{b}} > 230$ GeV	29.3	31.4	48.3	0.37
$z_{c.m.}^{\text{recon}}(b, \bar{b}) > 0.3$	13.0	21.7	4.5	0.50
$z_{c.m.}^{\text{recon}}(b, \bar{b}) > 0.3, z_{c.m.}^{\text{recon}}(H) < 0.5,$ and $M_{Wb\bar{b}} > 230$ GeV	10.8	9.2	2.5	0.92

at the cost of keeping only about 15% of the signal. A looser cut would not appreciably increase S/B , because of the top quark backgrounds. Provided one is willing to try the center-of-mass (c.m.) frame reconstruction, however, we show below that $z_{c.m.}^{\text{recon}}(b, \bar{b})$ (the cosine of the angle between b and \bar{b} quarks in the c.m. frame) can help to reduce the top backgrounds quite significantly as well. Here and below by the c.m. frame we mean the c.m. frame for the $W + b\bar{b}$ system.

Another reason to consider c.m. frame reconstruction is the strong potential of the observable $z_{c.m.}(H)$, which is the cosine of the polar angle of the Higgs boson in the $W + b\bar{b}$ center-of-mass frame. As discussed above, the t -channel-enhanced $W + X$ backgrounds are strongly peaked in the forward and/or backward region, while the signal is centrally peaked in the c.m. frame (see Fig. 2).

The angular distribution $z_{\text{lab}}(H)$ of the Higgs boson in the laboratory frame, shown in Fig. 3, is clearly much less informative, as a result of the washout by the longitudinal boost of the incoming partons. From Fig. 2 it is clear that a cut on $z_{c.m.}(H)$ can greatly reduce the $W + X$ backgrounds. Here, the challenge is to best reconstruct the leptonically decaying W boson, and then the c.m. reference frame, despite the indirect detection of the neutrino, the intrinsic width of the W boson, and limited detector resolution. The principal difficulty in

reconstruction stems from having to choose between the two solutions of the quadratic equation for the neutrino longitudinal momentum.

We have not attempted to find the optimal reconstruction algorithm, which we leave to more detailed studies. To merely point out the potential of our suggested c.m. frame cuts, however, we have selected the solution for the W boson lying closest in ΔR to the reconstructed Higgs boson. As is shown below, even this simple choice yields remarkable enhancement of S/B , which should motivate a more detailed study of the issue.

Thus reconstructing the c.m. frame, we obtain the observable $z_{c.m.}^{\text{recon}}(H)$, which approximates $z_{c.m.}(H)$, shown in Fig. 4 for the signal and backgrounds. Comparing to the cut in $\cos \Delta\phi(b, \bar{b})$, a cut in this variable manages to gain about the same increase in S/B , but at about 3 times as much in signal acceptance as before (Table VI). Further improvement is possible by including a cut on the total invariant mass, $M_{Wb\bar{b}}^2 = (p_W + p_{b\bar{b}})^2$. This is because of the fact that requiring a larger invariant mass $M_{Wb\bar{b}}$ somewhat improves the accuracy of our simple reconstruction algorithm, sharpening the $W + X$ forward and/or backward peak, and leaving proportionally more of the signal in the central region. With these two additional cuts (results given in Table VI), we have more than doubled the ratio of signal to $W + X$ backgrounds. The

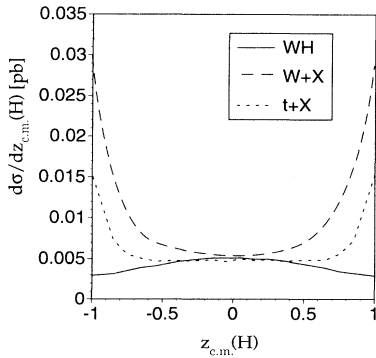


FIG. 2. The differential cross section $d\sigma/dz_{c.m.}(H)$ versus $z_{c.m.}(H)$ in the c.m. frame of $W + b\bar{b}$ for $M_t = 175$ GeV and $M_H = 100$ GeV at the LHC, for the signal (solid curve), the sum of W backgrounds (dashed curve), and the sum of top quark backgrounds (dotted curve). The acceptance cuts are according to scenario (ii).

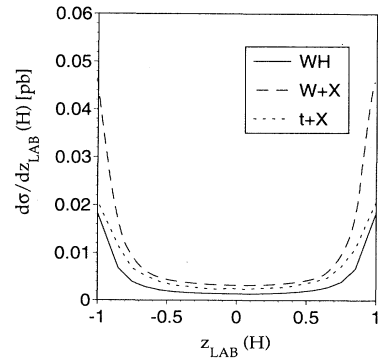


FIG. 3. The differential cross section $d\sigma/dz_{\text{lab}}(H)$ versus $z_{\text{lab}}(H)$ in the laboratory frame for $M_t = 175$ GeV and $M_H = 100$ GeV at the LHC, for the signal (solid curve), the sum of W backgrounds (dashed curve), and the sum of top quark backgrounds (dotted curve). The acceptance cuts are according to scenario (ii).

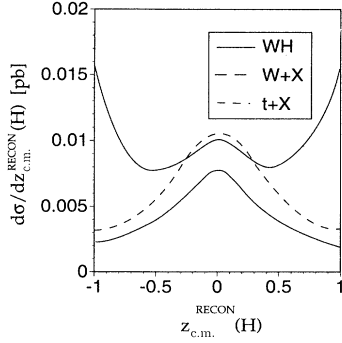


FIG. 4. The differential cross section $d\sigma/dz_{c.m.}^{\text{recon}}(H)$ versus $z_{c.m.}^{\text{recon}}(H)$ in the reconstructed c.m. frame of $W + b\bar{b}$ for $M_t = 175$ GeV and $M_H = 100$ GeV at the LHC, for the signal (solid curve), the sum of W backgrounds (dashed curve), and the sum of top quark backgrounds (dotted curve). The acceptance cuts are according to scenario (ii). Here the c.m. frame was reconstructed using the W boson solution nearest (in ΔR) to the reconstructed Higgs boson.

$z_{c.m.}^{\text{recon}}(H)$ cut is somewhat less efficient with respect to the top backgrounds, a fact which conversely may be useful in top quark *detection* above $W + X$ backgrounds [22]. Finally, we note that even without direct reconstruction of the $W + b\bar{b}$ rest frame, a less efficient version of this cut is possible by considering the *laboratory frame* double distribution in $(z_{\text{lab}}(H), z_{\text{lab}}(W))$ in which the $W + X$ background has peaks at (1,1) and (-1,-1) but not for the signal.

One can also differentiate between the signal and the backgrounds using $z_{c.m.}^{\text{recon}}(b, \bar{b})$, which is the cosine of the angle between the two bottom quarks in the c.m. frame of $W + b\bar{b}$. Figure 5 and Table VI show the efficacy of this observable in reducing the top backgrounds but less effective in reducing the W production backgrounds. This effect may be understood for the single-top-quark pro-

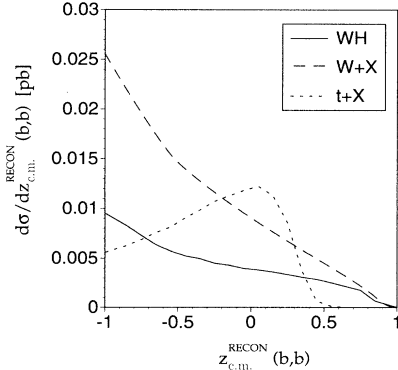


FIG. 5. The differential cross section $d\sigma/dz_{c.m.}^{\text{recon}}(b, \bar{b})$ versus $z_{c.m.}^{\text{recon}}(b, \bar{b})$ in the c.m. frame of $W + b\bar{b}$ for $M_t = 175$ GeV and $M_H = 100$ GeV at the LHC, for the signal (solid curve), the sum of W backgrounds (dashed curve), and the sum of top quark backgrounds (dotted curve). The acceptance cuts are according to scenario (ii). Here the c.m. frame was reconstructed using the W boson solution nearest (in ΔR) to the reconstructed Higgs boson.

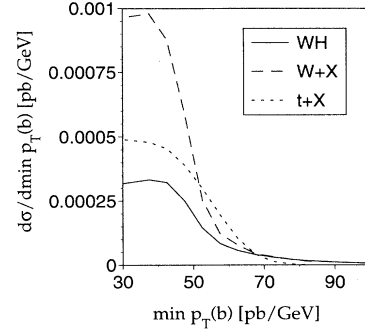


FIG. 6. The differential cross section $d\sigma/d[\min p_T(b)]$ versus the smaller of the transverse momenta of the two bottom quarks for $M_t = 175$ GeV and $M_H = 100$ GeV at the LHC, for the signal (solid curve), the sum of W backgrounds (dashed curve), and the sum of top quark backgrounds (dotted curve). The acceptance cuts are according to scenario (ii).

cesses, because in the c.m. frame the two bottom quarks tend to be produced in opposite hemispheres with respect to the plane transverse to the beam direction. Because this cut is somewhat orthogonal to that in $z_{c.m.}^{\text{recon}}(H)$, we have included the effects of applying both types of cuts in Table VI, which shows an overall increase in S/B by a factor of 4. Finally, we achieve a signal-to-background ratio close to 1:1.

Assuming the ability to reconstruct the W boson, it is natural to consider top reconstruction vetoes to reduce the top quark backgrounds. Reconstructing the W boson as described above, we have found that such a cut is possible, but because of the W boson and top quark widths, and especially detector resolutions, it is difficult to significantly increase the signal-to-background ratio.

Finally, Figs. 6 and 7 show that the bottom jets from the signal have relatively high p_T and energy, a fact which may be important in $m(b, \bar{b})$ resolution. In this study, we have assumed displaced-vertex tagging only of hadronically decaying bottom quarks, because the energy resolution of the leptonically decaying bottom quarks is degraded as a result of the presence of extra neutrinos.

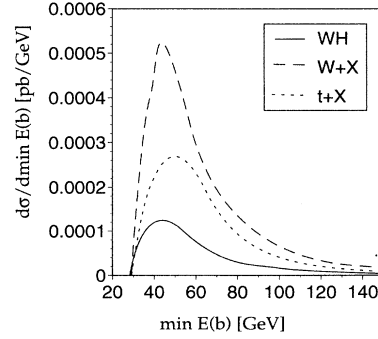


FIG. 7. The differential cross section $d\sigma/d[\min E(b)]$ versus the smaller of the energies of the two bottom quarks for $M_t = 175$ GeV and $M_H = 100$ GeV, for the signal (solid curve), the sum of W backgrounds (dashed curve), and the sum of top quark backgrounds (dotted curve). The acceptance cuts are according to scenario (ii).

Directly vetoing this decay mode is difficult, so that if necessary, requiring the jets to have higher energy and transverse momenta will help with angular and energy resolution of the jets, both by forcing the neutrino(s) to travel in the direction of the jet and also to soften leptonically decaying bottom jets.

V. DISCUSSION AND CONCLUSIONS

In this paper, we have studied the exclusive signature $e^\pm/\mu^\pm + b\bar{b}$ for the associated production of the Higgs boson with a mass in the lower intermediate mass region. Such a signature results through the process $pp \rightarrow WHX \rightarrow \ell\nu_\ell b\bar{b}X$. We considered the principal backgrounds and found that one can achieve fairly good observability for the signal. We have also studied a few strategies that one could adopt to enhance the signal-to-background ratio. For the sake of consistency, all processes were studied at LO; however, a brief study was carried out using PYTHIA to find the implications of NLO corrections.

We have studied two scenarios: optimistic and conservative. In both scenarios, we achieve fairly good statistical significance for the signal, a reasonable signal-to-background ratio, and a sufficient number of signal events. However, we also argue that because of potentially serious systematic errors it is advantageous to devise special cuts to further suppress the backgrounds. Given the very different nature of the production mechanisms for the signal and various backgrounds, it is natural to expect that a wide variety of observables exist that could help us in improving the signal-to-background ratio. We found that the observables $\Delta R(b, \bar{b})$ and $\cos \Delta\phi(b, \bar{b})$ in the laboratory frame and the observables $z_{c.m.}^{\text{recon}}(H)$ and $z_{c.m.}^{\text{recon}}(b, \bar{b})$ in the c.m. frame of the W boson and the $b\bar{b}$ pair, or a combination of them, are very useful in enhancing the signal-to-background ratio. Finally, we achieved the signal-to-background ratio close to 1 with about ten signal events for 10 fb^{-1} integrated luminosity.

Our goal was not to find the best set of cuts; this is best left for a study that includes detailed detector simulation. What we have shown is that the observation of the considered signature (or a variation) can lead to the detection of the Higgs boson if such a Higgs boson in the appropriate mass range exists. The variation of the signature that was briefly considered included the $e^\pm/\mu^\pm + b\bar{b}$ events with or without one (sufficiently soft) extra jet, with preliminary results obtained using PYTHIA.

The values of the statistical significance that we found are listed in Tables III and V. These results will certainly be degraded if the bottom-tagging efficiency or jet energy resolution are worse than our assumptions, which were motivated by the LOI of the ATLAS Collaboration and the technical design report of the SDC Collaboration. On the other hand, the integrated luminosity may well

be higher than what we have taken as a value, with obvious improvements in significance. Beyond collider and detector parameters, further improvements are possible in the cuts described above. Because, in general, strong correlations exist between such observables, one might suspect that optimal cuts should be placed in higher-dimensional scatter plots. Such tools as neural networks or decision trees [23] have obtained signal-to-background enhancements superior to conventional cuts.

In this study, we only use the electronic and muonic decays of the W boson. We have not considered the contribution of τ decay of the W boson and subsequent decay of the τ into an electron or muon. Such decays of the W boson will contribute to both the signal and the background. However, such contributions are expected to be small because of the inclusion of the further branching ratios of the τ into an electron or muon. Furthermore, these secondary electrons and muons are less energetic than the direct leptons from W decays, and therefore will have a lower acceptance rate.

So far, we have discussed only the standard model Higgs boson. In extensions of the standard model that have a larger Higgs sector, this mode can only be used in searching for the lightest neutral Higgs boson. The detectability of the lightest Higgs boson, using this associated production with a W boson and the decay of $Wh \rightarrow \ell\nu b\bar{b}$, depends on the WW_h and $hb\bar{b}$ couplings, which in turn depend on the parameter of the extended Higgs sector. For example, in the minimal supersymmetric standard model, the WW_h coupling is in general reduced from its standard model value, while the $hb\bar{b}$ is enhanced relative to the standard model value. So it remains possible to observe the lightest Higgs boson of the minimal supersymmetric standard model, but it will depend very much on the parameters of the model.

Finally, our focus was on the search of the Higgs boson at the LHC. For a search of the Higgs boson using the signature $e^\pm/\mu^\pm + b\bar{b}$ at the Tevatron, the major backgrounds to the signal are due to the $Wb\bar{b}$, WZ , and Wjj production. Our discussion of Sec. IV points out a few ways to reduce these backgrounds, e.g., by applying cuts on $\Delta R(b, \bar{b})$, $\cos \Delta\phi(b, \bar{b})$, or $z_{c.m.}(H)$ observables. Using a decision tree, one can use these or some other observables to find ways to enhance the signal with respect to the backgrounds [24].

ACKNOWLEDGMENTS

We are indebted to Duane A. Dicus for early participation and input. We would also wish to thank the following for useful discussions: H. Weerts, B. Pope, C. P. Yuan, J. Pumplin, G. Ladinsky, S. Willenbrock, and A. Stange. P.A. was supported in part by NSF Grant No. PHY-9396022. D.B.C. was supported in part by NSF Grant No. PHY-9307980. K.C. was supported in part by DOE Grant No. DOE-ER-40757-056.

- [1] CDF Collaboration, F. Abe *et al.*, Phys. Rev. D **50**, 2966 (1994).
- [2] ATLAS Letter of Intent, Report No. CERN/LHCC 92-4, 1992 (unpublished).
- [3] CMS Letter of Intent, Report No. CERN/LHCC 92-3, 1992 (unpublished).
- [4] E. Gross and P. Yepes, Int. J. Mod. Phys. A **8**, 407 (1993).
- [5] J.F. Gunion *et al.*, *The Higgs Hunter's Guide* (Addison-Wesley, Reading, MA, 1990).
- [6] J.F. Gunion, G.L. Kane, and J. Wudka, Nucl. Phys. **B299**, 231 (1988); V. Barger, G. Bhattacharya, T. Han, and B.A. Kniehl, Phys. Rev. D **43**, 779 (1991).
- [7] GEM Technical Design Report No. GEM-TN-93-262, 1993 (unpublished).
- [8] SDC Technical Design Report No. SDC-92-201, 1992 (unpublished).
- [9] Z. Kunszt, Z. Trocsanyi, and W.J. Stirling, Phys. Lett. B **271**, 247 (1991); W. Marciano and F. Paige, Phys. Rev. Lett. **66**, 2433 (1991); W.J. Stirling and D.J. Summers, Phys. Lett. B **283**, 411 (1992).
- [10] P. Agrawal and S. Ellis, Phys. Lett. B **229**, 145 (1989).
- [11] A. Stange, W. Marciano, and S. Willenbrock, Phys. Rev. D **49**, 1354 (1994); **50**, 4491 (1994), and references therein.
- [12] T. Garavaglia, W. Kwong, and D. Wu, Phys. Rev. D **48**, R1899 (1993); J. Dai, J. Gunion, and R. Vega, Phys. Rev. Lett. **71**, 2699 (1993).
- [13] See, e.g., OPAL Collaboration, R. Akers *et al.*, Z. Phys. C **61**, 209 (1994).
- [14] S.D. Ellis, R. Kleiss, and W.J. Stirling, Phys. Lett. **154B**, 435 (1985).
- [15] D0 Collaboration, S. Abachi *et al.*, Phys. Rev. Lett. **72**, 2138 (1994).
- [16] T. Han and S. Willenbrock, Phys. Lett. B **273**, 167 (1991); J. Ohnemus and W.J. Stirling, Phys. Rev. D **47**, 2722 (1993); H. Baer, B. Bailey, and J.F. Owens, *ibid.* **47**, 2730 (1993).
- [17] P. Agrawal, J. Qiu, and C.P. Yuan, Report No. MSU-HEP-93-8 (unpublished); in *Proceedings of the Workshop on Physics at Current Accelerators and the Supercollider*, Argonne, Illinois, 1993, edited by J.L. Hewett *et al.* (ANL Report No. 93-92, Argonne, 1993).
- [18] P. Nason, S. Dawson, and R.K. Ellis, Nucl. Phys. **B303**, 607 (1988); W. Beenakker, H. Kuijf, W.L. Neerven, and J. Smith, Phys. Rev. D **40**, 54 (1989).
- [19] T. Sjöstrand, Comput. Phys. Commun. **39**, 347 (1986); T. Sjöstrand and M. Bengtsson, *ibid.* **43**, 367 (1987).
- [20] CTEQ Collaboration, J. Botts *et al.*, Phys. Lett. B **304**, 159 (1993).
- [21] P. Agrawal, D. Bowser-Chao, K. Cheung, and D. Dicus, in Proceedings of Meeting of the Division of Particles and Fields of the APS, Albuquerque, New Mexico, 1994 (unpublished).
- [22] P. Agrawal, D. Bowser-Chao, and J. Pumplin, Report No. MSU-HEP/50327 (unpublished).
- [23] D. Bowser-Chao and D. Dzialo, Phys. Rev. D **47**, 1900 (1993).
- [24] P. Agrawal, D. Bowser-Chao, and J. Hughes, Report No. MSU-HEP/50515 (unpublished).